Antecedent Conditions Mitigate Carbon Loss During Flash Drought Events

Nicholas Parazoo[1], Mahmoud Osman[2,3], Madeleine Pascolini-Campbell[1], Brendan Byrne[1]

[1]Jet Propulsion Laboratory, California Institute of Technology, Pasadena, CA, USA
[2]Department of Earth and Planetary Sciences, Johns Hopkins University, Baltimore, MD, USA
[3]Irrigation and Hydraulics Department, Cairo University, Cairo, Egypt

Corresponding author: Nicholas Parazoo (nicholas.c.parazoo@jpl.nasa.gov)

Key Points:

- SIF offers early warning (~2-3 months) for stealth drought events.
- Pre-drought carbon gains fully offset post-drought carbon loss.
- Terrestrial biosphere models overestimate total carbon loss.

Abstract

Flash droughts– the rapid drying of land and intensification of drought conditions - have devasting impacts to natural resources, food supplies, and the economy. Less is currently known about the drivers of flash droughts and their impact to landscape carbon losses. We leverage carbon and water cycle data from NASA OCO-2 and SMAP missions to determine the net impact of flash drought events in the U.S. on the carbon sinks. On average, pre-onset carbon uptake fully offsets post-onset losses, creating a carbon neutral biosphere over a ± 3 month period surrounding flash drought onset. This contrasts with ecosystem models, which underestimate pre-onset uptake and overestimate post-onset loss. Furthermore, spaceborne observations of solar induced fluorescence (SIF) provide a reliable indicator of flash droughts at lead times of 2-3 months, due to feedbacks between vegetation growth and soil water loss. This study is expected to improve understanding and prediction of flash droughts.

Plan Language Summary

Flash droughts have devasting impacts to the environment, natural resources, and society, and are difficult to predict. Here, we use NASA models and satellite observations to determine (1) the impact of flash drought on storage of carbon in land ecosystems, and (2) the extent to which satellite remote sensing can improve flash drought early warning. We find that beneficial environmental conditions occurring prior to onset of flash drought leads to increases in carbon storage in ecosystems compared to normal conditions. This anomalous storage of carbon in ecosystems is sufficient to fully offset inevitable decreases in carbon storage associated with hot dry conditions following onset of flash drought, leading to a net zero impact of flash drought on carbon storage over the 6-month period surrounding drought onset. Moreover, we find the satellite observations of solar induced chlorophyll fluorescence (SIF), representing a re-emission of radiation by plants following absorption of sunlight for growth, are extremely well correlated to soil moisture losses associated with flash drought at lead times of 6-12 weeks across diverse landscapes and ecoregions in North America. Satellite SIF thus shows promise as a reliable early warning indicator of flash drought, at sufficient lead time conducive to decision making.

1. Introduction

Flash droughts have been responsible for some of the most damaging droughts in the United States in the past decade [*Zhang and Yuan, 2020*]. The rapid emergence and onset of land drying and vegetation stress often results in significant damage to natural and managed vegetation [*Zhang and Yuan, 2020*], which has direct and immediate impacts to natural resources, food supplies, and the economy [*Otkin et al., 2018*]. These events can also have important downstream impacts to carbon storage through changes in photosynthetic uptake, soil respiration, and elevated fire risk [*Wolf et al., 2016; Hoell et al., 2019*]. However, the extent to which these events drive anomalous carbon loss is unknown due to the large range of seasonal timing, geographical location, land cover, land use, and drought severity. As such, despite extensive assessment of meteorological drought impacts on vegetation and carbon [e.g., *Ciais et al., 2005; Parazoo et al., 2015; Wolf et al., 2016; Madani et al., 2020*], relatively little is currently known about the impact of these short-term extremes on carbon storage.

Flash droughts have also been difficult to predict and monitor [*Chen et al., 2019; Ford and Labosier, 2017; Pendergrass et al., 2020*], in part due to the absence of significant precipitation deficits characterizing more traditional meteorological droughts. Flash droughts are triggered or exacerbated by high temperatures leading to increased evaporative demand, often appearing suddenly and without warning, and can persist weeks to months [*Anderson et al., 2013; McEvoy et al., 2016; Otkin et al., 2013, 2018*]. The limited predictability, the potential for significant impacts to natural resources, carbon storage, and water resources, and the apparent link to high temperatures have motivated efforts to inventory, monitor, and forecast flash drought events [*e.g., Mo and Lettenmaier, 2015, 2016; Ford and Labosier, 2017; Osman et al., 2021, 2022*].

Osman et al (2021, 2022) developed a soil moisture volatility-based flash drought definition to inventory flash drought onset and severity across the Contiguous United States (CONUS) over 4 decades. Critically, this work demonstrates the universal signature of soil moisture anomalies across thousands of flash drought events, and frequent absence of severe precursor meteorological anomalies. This inventory provides a unique opportunity to study the impact of flash drought on carbon exchange, and evaluate new precursors for flash drought.

In addition, spaceborne observations of solar induced fluorescence (SIF) have also proven to be a useful tool for monitoring flash droughts (*Mohammadi et al., 2022*), as SIF exhibit unusually fast responses to drought, providing lead time of 2 weeks to 2 months for flash drought onset. The rapid physiological changes tracked with SIF contrast with the more structural responses tracked by Normalized Difference Vegetation Index (NDVI), the Enhanced Vegetation Index (EVI), which are among the many drought indicators currently used by the US Drought Monitor (USDM).

Improving detection and characterization of flash droughts and understanding how they impact ecosystem carbon and water budgets will be critical as flash droughts become more common [*Yuan et al., 2023*]. This study builds on recent developments in remote sensing and flash drought inventories to (1) determine the extent to which spaceborne SIF provides an advanced indicator of flash drought across multiple classes, vegetation types, and regions, and (2) quantify the temporally and spatially integrated impact of flash droughts on carbon and water budgets. We leverage gridded estimates of ecosystem carbon exchange, vegetation productivity and evapotranspiration, soil moisture, and atmospheric forcing using products constrained by satellite (OCO-2, SMAP, MODIS) and ground-based (NOAA CO_2 Network) observational data. Time series of these products are sampled against flash drought inventories over the CONUS from 2015-2020, and analyzed over a period of ± 3 months relative to date of drought onset. We examine patterns of variability in space and time, across drought classes, ecoregions, and vegetation types. Our objective is to describe the cascade of events in the atmosphere, land, and soil leading to soil moisture loss and changes in carbon uptake, which will improve our understanding of drought, and advance drought forecasting and carbon cycle projections.

2. Methods

2.1 Flash Drought Inventory

We leverage the inventory of soil moisture flash droughts generated and extended by *Osman et al (2021*, *2022*) for CONUS from 1979–2021 at 0.125° spatial resolution. Flash droughts are identified using a soil moisture volatility index (SMVI) calculated using root zone soil moisture (RZSM) from the NLDAS-2 soil moisture dataset (https://ldas.gsfc.nasa.gov/nldas/v2/forcing). SMVI captures change that is more rapid than usual and is thus ideally suited for both rapid onset and rapid intensification drought events. Flash drought onset is recorded when 1) the 5-day RZSM moving average falls and stays below the 20-day moving average for at least 20-day days or 2) both simple moving averages are below the 20th percentile of the 1979–2020 time-of-year RZSM climatology (*Osman et al. 2021*). We examine patterns of carbon, water, and meteorological variables for three categories of flash drought produced from this inventory, defined based on the magnitude of precursor meteorological anomalies: (1) “stealth”, which are least severe in terms of evaporative demand and soil moisture, (2) "dry and demanding" which are most severe with high evaporative demand and low soil moisture, and (3) "evaporative" with modest evaporative demand and soil moisture anomalies.

2.2 Carbon Cycle Data

Net Ecosystem Exchange: Atmospheric CO_2 inversions use data assimilation methods to adjust prior estimates of natural CO_2 flux from terrestrial biosphere models into agreement with observed spatial and temporal gradients in atmospheric CO_2. The amount of adjustment depends on uncertainty applied to the models and observations, as well as the sensitivity of observations to surface fluxes. The v10 Orbiting Carbon Observatory (OCO-2) Model Intercomparison Project (v10 OCO-2 MIP) accounts for differences in observational constraint and prior flux, by performing an ensemble of inversions using different models as priors and different combinations of CO_2 data from the OCO-2 satellite (land nadir + land glint, LNLG) and surface sites (*in situ*, IS). We leverage 1° x 1° ensemble mean posterior fluxes from v10 OCO-2 MIP inversions (*Byrne et al., 2023* and references therein) constrained by combined spaceborne and in situ observations (LNLGIS), which extend from the beginning of the OCO-2 record in January 2015 through December 2020 (denoted posterior NBP). We also examine model priors for comparison (denoted prior NBP). Monthly fluxes are downscaled to weekly resolution using spline interpolation.

Solar Induced Fluorescence: SIF remote sensing measurements capture seasonal, interannual, and long term variability in vegetation growth across dryland and forested ecosystems in North America [*Parazoo et al., 2014; 2015; Smith et al 2018*]. OCO-2 measures SIF at high precision and accuracy, and small spatial footprint (1.3 x 2.25 km^2), needed to capture vegetation feedbacks with water and carbon. However, it's narrow OCO-2 swath (10 km) and infrequent repeat frequency (16 days) limits studies of rapid change associated with flash drought. Methods have been applied to downscale OCO-2 SIF products using MODIS reflectance (e.g. CSIF; *Zhang et al 2018*) and the combination of MODIS reflectance and meteorological data (GOSIF; *Li and Xiao 2019*). These methods use machine learning algorithms to extrapolate, upscale and fill the gaps in OCO-2 SIF retrievals, providing gridded SIF datasets at 4-day 5 km resolution from 2001-2020 (CSIF v2) and 8-day 5 km resolution from 2001-2022 (GOSIF). We leverage CSIF and GOSIF products as baseline drought indicators, preprocessed into 4-day and 8-day averages, respectively, for the period 2015-2020 in alignment with v10 OCO-2 MIP fluxes.

2.3 Water Cycle Data

Soil Moisture: The NASA Soil Moisture Active and Passive (SMAP) satellite mission is used to track daily changes in soil water during flash drought development. SMAP Level 4 derived soil moisture products are produced from merging SMAP L3 soil moisture data with land surface models of water, energy, and carbon (*Reichle et al., 2019*). We use daily 9 km estimates of surface and root zone soil moisture from NSIDC.

Evapotranspiration: The Global Land Data Assimilation System (GLDAS) is used to track daily changes in evapotranspiration (ET) for feedbacks to atmospheric demand. GLDAS V2.2 uses advanced land surface modeling and data assimilation techniques to generate global optimal fields of land surface states and fluxes at daily 0.25° x 0.25° (*Rodell et al., 2004*).

2.4 Meteorological Data

Meteorological fields including daily vapor pressure deficit (VPD), air temperature, and water vapor are taken from hourly MERRA-2 reanalysis at 0.67° x 0.5°. Precipitation is taken from the GPCP V3.2 daily product.

2.5 Analysis

We analyze carbon and water cycle responses over a ± 3 month period surrounding drought onset. We limit our analysis to flash drought events with onset dates from May-July, such that our effective analysis period spans late winter (February) through fall (October), inclusive of longer growing seasons in southern CONUS, while excluding the dormant season for most of CONUS. We examine a total of 32,211 events occurring from May-July in CONUS, spanning the period 2015-2020. We examine multiple drought categories, ecoregions (Fig S1) and land cover (Fig S2). Ecoregions are based on Bukovsky regions representing climatically homogenous regions in CONUS (*Bukovsky, 2011*). Land cover is based on aggregated plant functional types from the International Geosphere-Biosphere Project (IGBP).

All carbon, water, meteorological, and vegetation datasets are sampled at the nearest time and location of onset from the flash drought inventory from 2015-2020. Spatial analysis is conducted by aggregating across similar vegetation or flash drought categories, using the area average for each event (area average varies per dataset). Temporal analysis is conducted using Z-scores with mean and standard deviation computed over 1-8 day windows (depending on the product) from 2015-2020. Uncertainties are computed as standard errors.

v10 OCO-2 MIP inversions solve for natural fluxes (net biosphere exchange, NBE), representing the sum of fire emission (Fire) and net ecosystem exchange (NEE). NBE represents net exchange from land to atmosphere, with positive values indicating net source and negative values a net sink. We use the GFED4.1s fire emissions dataset (*Giglio et al., 2013; van der Werf et al., 2017*) to determine the contribution of fires to NBE.

For the primary analysis, we exclude flash droughts accompanied by fires with emissions exceeding 0.001 g C m^{-2} yr^{-1}. These events are widespread and have significant pre- and post-onset influence (See Text S1 and Figs S3-S5). This reduces the final sample size to 23,825. We include this small threshold to keep the sample size sufficiently high, which would otherwise reduce to 4,025 samples if all fires events were excluded (N = 3806).

3. Results

The temporal distribution of spatially aggregated NBE standardized anomalies (i.e., mean response across all flash drought events) is characterized by net carbon uptake (or gain) prior to drought onset, and net carbon emission (or loss) following drought onset (Figure 1). Peak uptake occurs 6-8 weeks before onset, following positive anomalies in SIF (6-12 weeks prior to onset), and gradually becomes a weaker sink with declining SIF and soil moisture. The transition from net sink to net source occurs approximately at onset, following rapid declines in soil moisture and SIF. Peak efflux occurs 4-5 weeks after onset, 1-2 weeks after the peak negative anomaly in SIF.

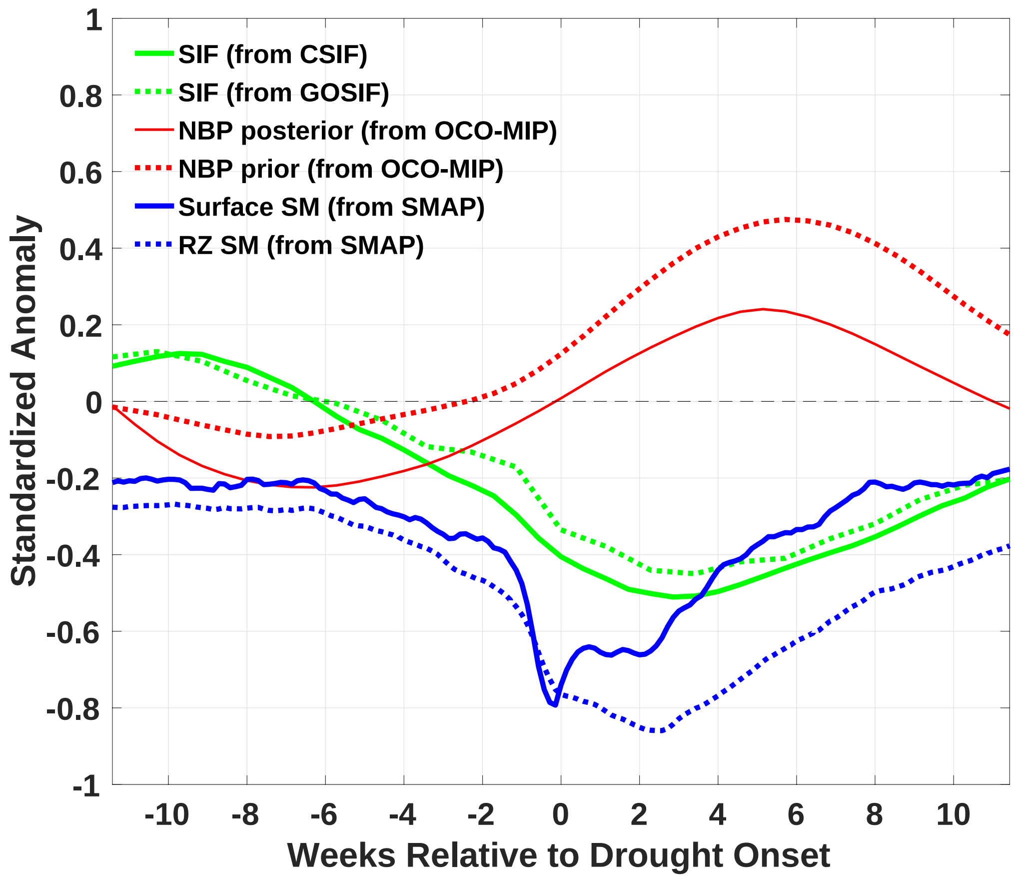

Figure 1. Standardized anomalies (Z-score) of solar induced fluorescence (SIF), net biome production (NBP), and soil moisture during flash drought events. Anomalies represent the ensemble average of events in CONUS occurring in May-July from 2015-2020. Negative values of NBP indicate net uptake, and positive values net efflux. Two SIF-based proxies of photosynthesis (green, GOSIF and CSIF) show positive anomalies 6-12 weeks prior to drought onset (x = 0), which is synchronized with negative anomalies of NBP (solid red, constrained by atmospheric CO2 observations) and negative anomalies of surface and root zone soil moisture (dashed and solid blue lines, respectively). NBP and SIF patterns are reversed following drought onset. NBP priors, representing model-based estimates unconstrained by atmospheric CO2 (dashed red), underestimate pre-drought uptake and thus overestimate total flash drought carbon losses.

In general, these temporal patterns are consistent across SIF products (CSIF and GOSIF), soil moisture profiles (root zone and surface), and NBE estimates (prior and posterior). An important exception is the persistent positive offset in prior NBE (dashed, unconstrained), which is characterized by a weak net sink prior to onset and strong net source afterward. Consequently, posterior estimates of temporally integrated standardized anomalies (Fig S6 and Table S1) show approximately zero net carbon loss on average (mean Z-score = -0.006 ± 0.00097), with prior estimates suggesting an anomalous source (mean Z-score = 0.17 ± 0.00095). CO_2 observational constraints thus impose strong pre-drought increases in sink strength (mean Z-score = -0.14 ± 0.0014) which are unaccounted for in model priors, and which fully offset post-drought reductions in sink strength (mean Z-score = 0.13 ± 0.0013). While there are many cases of pre-drought carbon gain in prior estimates (Fig S6B), they are less frequent and less skewed toward negative values compared to posterior estimates (Fig S6A). The NBE response shifts toward an anomalous source when including scenarios in which flash drought is accompanied by fires (Text S1, Fig S7, Table S1).

The spatial distribution of temporally integrated standardized anomalies indicates a mixed pattern of net carbon sink anomalies (blue) and net source anomalies (red) across CONUS from 2015-2020 (Figure 2). In general, source anomalies, which are most prevalent in southern areas, are partially offset by sink anomalies in northern areas. This spatial pattern is related to regional difference in climate and vegetation. For example, the North America Desert ecoregion (Fig S8D) shows a persistent net source anomaly over the entire flash drought period (± 3 months surrounding onset). This region is dominated by semi-arid vegetation including shrubs and savannah, which show similar pre- and post- onset responses (Fig S9C-D) and is prone to negative soil moisture and SIF anomalies early on. The Eastern Temperate Forest ecoregion (Fig S8B), on the other hand, shows a weaker but more prolonged period of drawdown extending beyond drought onset. This region shows minimal soil moisture loss early on, and negligible reductions in SIF compared to other regions. The contrasting response between Western Desert and Eastern Forest regions is potentially related to differences in water limitations and dominant flux component controls, with dry region sinks more susceptible to drought induced GPP declines, and wetter eastern forests more susceptible to drought induced respiration declines following rapid soil moisture loss 4 weeks prior to onset. This result is also consistent with increased pre-drought productivity being strongest in regions where spring productivity is temperature limited (*Byrne et al., 2020*). NW Forest and Great Plain ecoregions (Fig S8A,C) show patterns more characteristic of the mean CONUS signal, including pre-onset sink and positive SIF anomalies, and post-onset source and negative SIF anomalies.

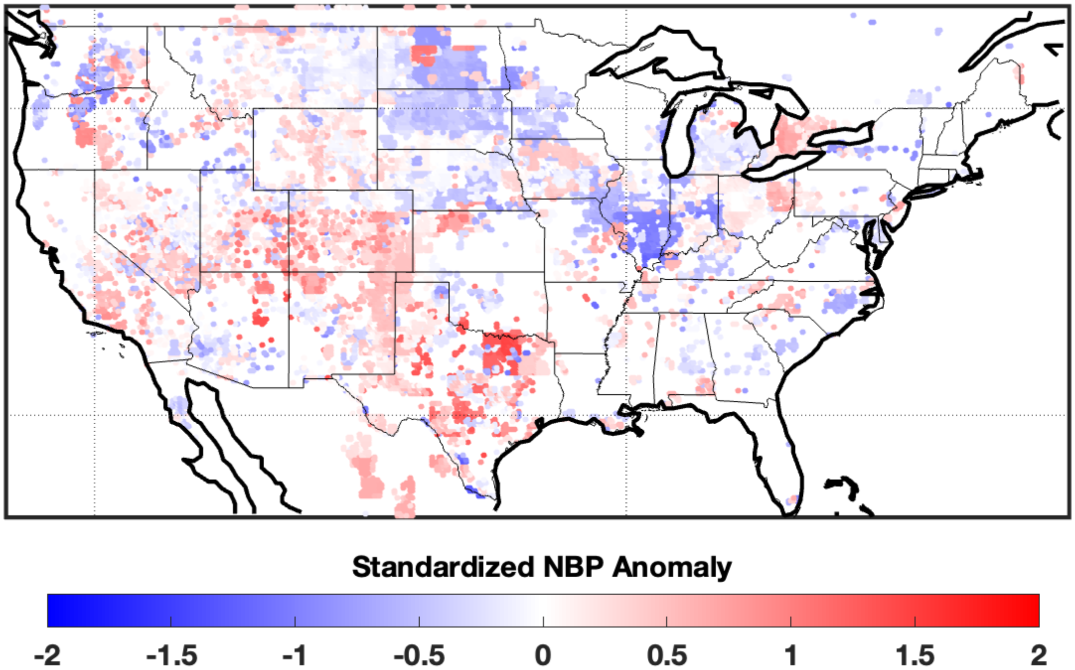

Figure 2. Spatial distribution of standardized NBP anomalies for flash drought events in Figure 1. Blue shading indicates net uptake of carbon; red shading indicates net efflux of carbon. The multi-event average is shown for pixels in which multiple events occurred from 2015-2020.

Several ecoregions (NW Forests, Great Plains) and vegetation classes (Needleleaf Evergreen Forest, Grassland, and Cropland) show positive anomalies of SIF at lags of 4 -12 weeks prior to drought onset, suggesting a boost to plant productivity several months prior to onset of flash drought. This raises the question as to whether increased drawdown of soil water due to enhanced plant growth contributes to the development of flash drought.

To answer this question, we perform lag correlation analysis of SIF and ET versus surface soil moisture at lags of 0 to 15 weeks (Figure 3). Our results show that SIF is negatively correlated with soil moisture at lags of 8-15 weeks for all drought classes, with timing and value of peak negative correlation as follows: 8 weeks for "Evaporative" droughts (r = -0.95), 10-11 weeks for "Stealth" droughts (r = -0.90), and 11 weeks for "Dry and Demanding" drought (r = -0.98). A similar analysis of ET and soil moisture shows strong negative correlation peaking at 8 week time lag for Evaporative droughts and no correlation under Stealth droughts.

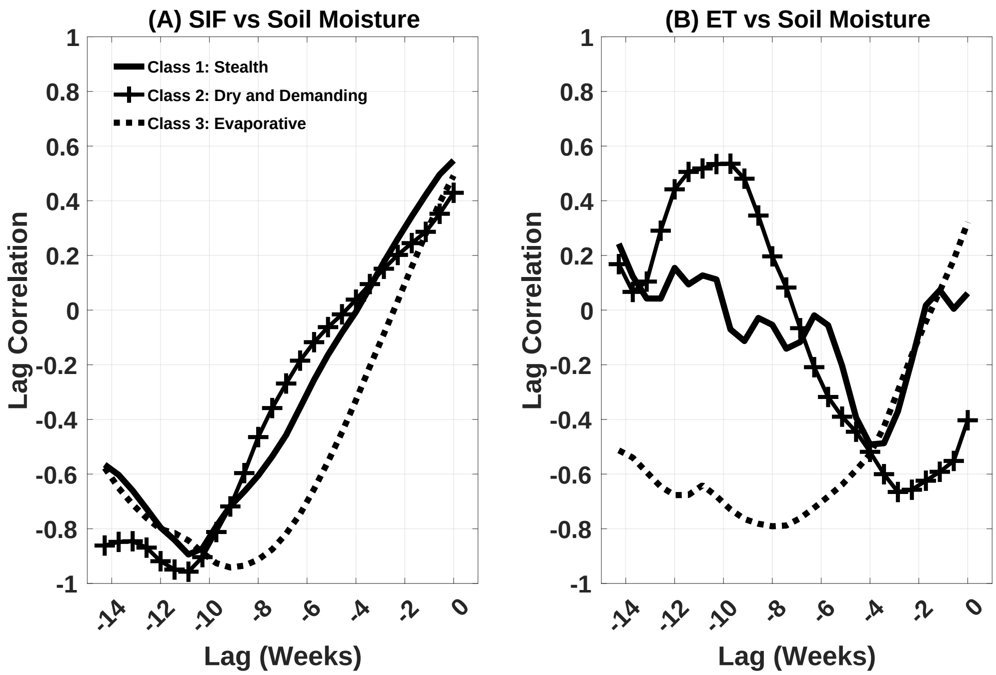

Figure 3. Lag correlation between standardized anomalies of vegetation properties and surface soil moisture. Results are shown for (A) solar induced fluorescence (SIF) vs soil moisture, and (B) evapotranspiration (ET) vs soil moisture, and partitioned into flash drought categories including Stealth (solid), Dry and Demanding (solid + crosses), and Evaporative (dashed). Correlations are shown in increments of one week from 0 to 15 weeks before drought. Negative lags indicate the vegetation properties lead soil moisture in time.

Moreover, standardized SIF anomalies are consistently positive at lags of 6-12 weeks prior to onset (Fig S10). Peak Z-score values exceed zero in 80% of flash drought cases, with lowest rates in "Dry and Demanding" droughts (76%) and highest rates in "Evaporative" droughts (83%). The median anomaly is significant for each drought category, ranging from 0.69 for "Stealth Drought" to 0.85 for "Evaporative" droughts.

Vegetation productivity and soil moisture thus appear to be strongly coupled under antecedent conditions associated with flash drought, with soil moisture responding to variations in SIF 2-3 months earlier. Similar patterns emerge across ecoregions (Fig S11) and vegetation classes (Fig S12), especially under Stealth drought conditions, and including managed land cover (Fig S12F) and desert ecoregions (Fig S11D).

Standardized SIF anomalies thus appear to provide a reliable indicator of flash drought across diverse ecoregions, vegetation types, and drought classes, at long lead times (6-12 weeks), with fairly low false-positive rate (~20%) and strong signal (Median Z-Score of 0.75).

4. Discussion and Conclusions

Aggregating SIF and CO_2 flux anomalies across all flash drought events in CONUS from 2015-2020 shows a systematic response of the terrestrial biosphere to flash drought, characterized by (a) an increase in SIF, photosynthesis, and net drawdown of CO_2 before drought onset, (b) gradual depletion of soil water, (c) transition toward net efflux of carbon with declining photosynthesis and soil water, (d) shift to net source with sudden loss of soil moisture 1-2 weeks prior to drought onset, and (e) peak efflux of carbon at 4-5 weeks after onset.

4.1 Cascade of Events

The cascade of meteorological, carbon cycle, and soil moisture events is depicted in Figure 4. Beneficial warm antecedent conditions 10-12 weeks prior to drought onset stimulate anomalous vegetation activity 6-12 weeks prior to drought onset. Persistent warming and drying of the land surface (increased air temperature and atmospheric demand) 6-12 weeks out drives gradual boundary layer growth 2-8 weeks out, which exacerbates dry conditions. The combined effects of warming, drying, and vegetation growth deplete soil moisture at the surface and in the root zone. Finally, extreme hot, dry conditions 1 week out triggers abrupt decreases in soil moisture leading to onset of flash drought and post drought carbon losses.

This "Cascade of Events" is consistent with mounting evidence that hot-dry extremes can initially benefit vegetation by stimulating growth under temperature limiting conditions, for example in spring in temperate latitudes, and following snow melt in high latitudes and altitudes [*Ciais et al., 2005; Wolf et al., 2013; 2016; Keenan et al., 2014; Madani et al., 2021*]. While this can initially increase photosynthesis and carbon storage, vegetation feedbacks can exacerbate hot-dry extremes by depleting soil water taken up by roots for photosynthesis and lost through transpiration. The combination of vegetation feedbacks with heightened atmospheric demand accelerates soil water depletion, providing a potential mechanism for rapid onset of drought (i.e., flash drought) and subsequent reductions in carbon uptake related to stomatal closure (to conserve water) and decreased productivity.

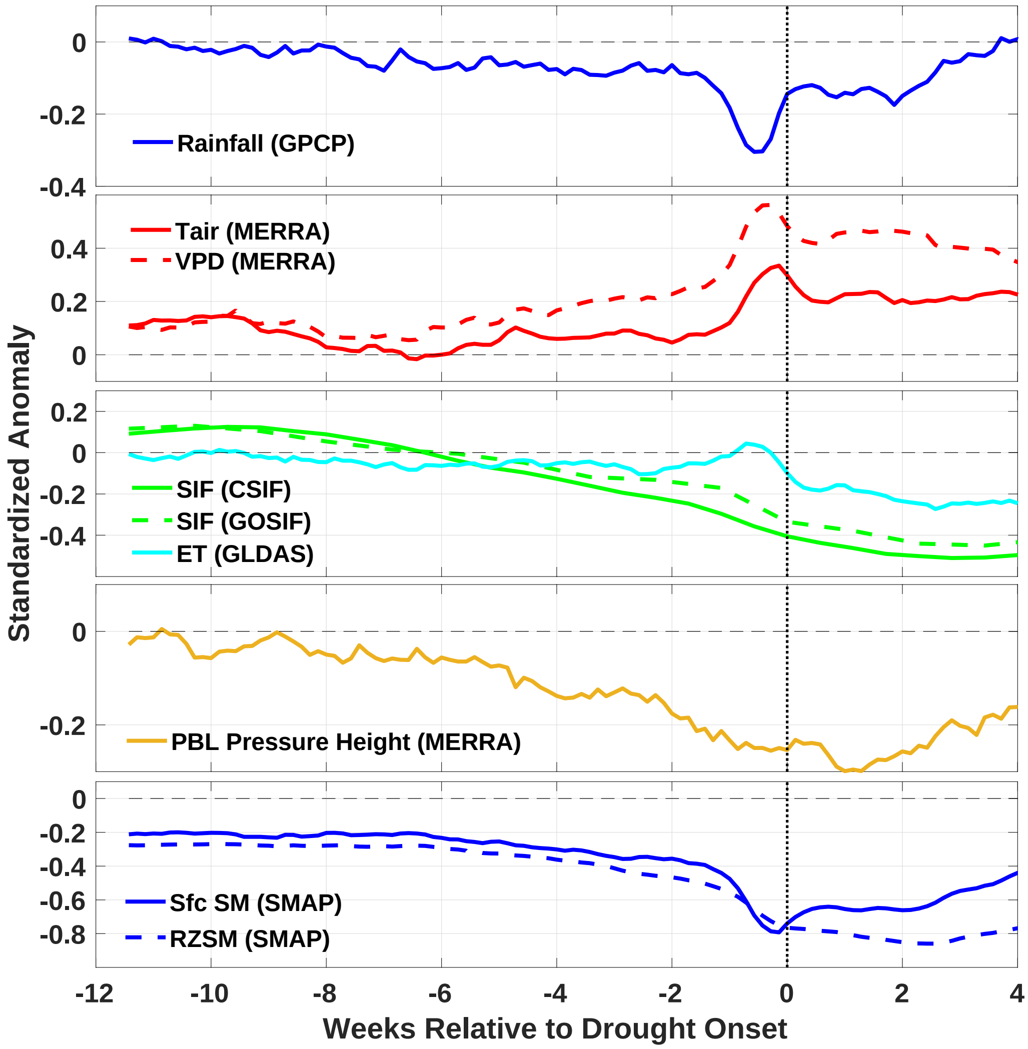

Figure 4. "Cascade of events" depicted by standardized anomalies of meteorological, vegetation, atmospheric, and soil moisture variables during "Stealth" flash drought events. Beneficial wet and warm antecedent conditions 10-12 weeks prior to drought onset (A-B) stimulate anomalous vegetation activity 6-12 weeks prior to drought onset (C). Persistent warming and drying 6-12 out (B) drives boundary layer growth 2-8 weeks out (D). The combined effects of warming, drying, and vegetation growth lead to gradual depletion of soil moisture at the surface and in the root zone (E). Extreme hot, dry conditions precede flash drought onset.

4.2 Net Zero Carbon Response

Pre- and post-drought onset NBE standardized anomalies (Z-score = -0.14 and 0.13 on average, respectively) largely cancel out, producing a negligible carbon sink anomaly (-0.006) across all flash drought events. In projecting carbon responses to future extremes, it is therefore critical to account for the integrated response before and after drought onset. Recent work looking at carbon cycle responses to future extremes indicate the dominance of negative carbon anomalies (*Sharma et al., 2023*). NBE anomalies from this study were computed for lags of 1-4 following onset of climate extremes. By not accounting for pre-drought anomalies, future carbon losses are likely overestimated. We acknowledge that carbon response patterns may shift in the future with more frequent and intense extremes; nevertheless, our study highlights that integrated effects are non-negligible.

As flash droughts become more common [*Yuan et al., 2023*], accurate assessments of drought inventories and carbon and water cycle impacts will be critical. V10 OCO-2 MIP priors used in this analysis strongly underestimate carbon uptake associated with beneficial antecedent conditions, and overestimate emissions after drought onset. This supports previous studies that show poor performance in representing ecosystem response to drought [*Byrne et al., 2020; Kolus et al., 2019*]. Our analysis highlights several areas of focus to improve model representations of drought-carbon interactions: (1) temperature sensitivity of photosynthesis across diverse ecosystems to abnormally warm springs, (2) plant-soil water interactions which can sustain photosynthesis while depleting soil moisture, and (3) sensitivity of heterotrophic respiration to abrupt warming and drying.

4.3 SIF is a Promising Early Warning Indicator of Flash Drought

These findings illustrate the value of spaceborne SIF for flash drought early warning especially for events occurring in early to mid-summer, providing reliability in terms of strong signal and low false-positivity rate. Significant positive anomalies in standardized SIF are a frequent occurrence ahead of flash drought (median Z-score = 0.80) and are extremely well correlated to negative soil moisture anomalies at lags of 2-3 months. Stealth droughts in particular are challenging to forecast due to reduced severity of meteorological indicators and could easily benefit from tracking standardized SIF anomalies early on.

Several key factors that continue to hinder full implementation of spaceborne SIF within drought forecasting systems such as the US Drought Monitor are data latency, frequency, and coverage. OCO-2 provides accurate tracking of the mean response across multiple events, but individual events or spatial gradients are hidden by infrequent (16-day) and sparse (8 km swath) sampling. SIF enabled sensors such as GOME-2 and TROPOMI provide improved mapping and early warning of drought events (e.g., *Mohammadi et al., 2022*), but are currently not produced operationally. Furthermore, coarse footprints comprising the program of record (5 – 50 km) do not resolve mixed land cover including managed systems (< 1 km) masking critically important flash drought impacts on crop yield and food security, and other potential buffers (or amplifiers) to carbon flux anomalies. Irrigation, which was not analyzed here, is likely to have an important influence on flash drought responses. Continued research is needed to better understand the link between SIF and meteorological factors on the timing, magnitude and duration of drought, and more emphasis should be placed on collaborative work between drought forecasting agencies and research institutions. We also recommend parallel efforts focused on more operational use of SIF through reduced data latency, implementation of near real time data fusion systems to produce gridded maps with moderate temporal resolution (~4-8 days), and development of wide swath satellite sensors capable of producing spatially resolved maps of SIF at high frequency.

Acknowledgements

The research was carried out at the Jet Propulsion Laboratory, California Institute of Technology, under a contract with the National Aeronautics and Space Administration (80NM0018D0004). The authors acknowledge support from the NASA Earth Science Division and the Orbiting Carbon Observatory 2 Mission.

Open Research

Data products used in this analysis are openly available as follows: Flash drought inventory (https://github.com/mosman01/SMVI/tree/main/SMVI_NLDAS_E1_E2); v10 OCO2 MIP NBP ((https://www.gml.noaa.gov/ccgg/OCO2_v10mip/); GFED4.1s Fire Emissions (https://www.geo.vu.nl/~gwerf/GFED/GFED4/); GOSIF SIF (https://globalecology.unh.edu/data/GOSIF.html); CSIF SIF (https://osf.io/8xqy6/); MERRA-2 air temperature, VPD, and atmospheric moisture (https://gmao.gsfc.nasa.gov/reanalysis/MERRA-2/); GPCP Precipitation (https://disc.gsfc.nasa.gov/datasets/GPCPDAY_3.2/summary); SMAP Soil Moisture (https://nsidc.org/data/smap); GLDAS ET (https://ldas.gsfc.nasa.gov/gldas); Bukovsky ecoregions (https://www.narccap.ucar.edu/contrib/bukovsky/); MODIS IGBP land cover (https://modis.gsfc.nasa.gov/data/dataprod/mod12.php).

References

Anderson, M. C., C. Hain, J. A. Otkin, X. Zhan, K. Mo, M. Svoboda, B. Wardlow, and A. Pimstein, 2013: An intercomparison of drought indicators based on thermal remote sensing and NLDAS simulations. J. Hydrometeor., 14, 1035–1056,

Bukovsky, M. S. (2011). Masks for the Bukovsky regionalization of North America. http://www.narccap.ucar.edu/contrib/bukovsky/.

Byrne, B., Liu, J., Bloom, A.A., Bowman, K.W., Butterfield, Z., Joiner, J., Keenan, T.F., Keppel-Aleks, G., Parazoo, N.C. and Yin, Y., 2020. Contrasting regional carbon cycle responses to seasonal climate anomalies across the east-west divide of temperate North America. *Global biogeochemical cycles*, *34*(11), p.e2020GB006598

Byrne, B., Liu, J., Lee, M., Yin, Y., Bowman, K. W., Miyazaki, K., et al.(2021). The carbon cycle of southeast Australia during 2019–2020: Drought, fires, and subsequent recovery. AGU Advances, 2, e2021AV000469.Byrne et al., 2023

Chen, L. G., Gottschalck, J., Hartman, A., Miskus, D., Tinker, R., & Artusa, A. (2019). Flash Drought Characteristics Based on U.S. Drought Monitor. Atmosphere, 10(9), 498. https://doi.org/10.3390/atmos10090498Ciais et al., 2005

Ford, T. W., & Labosier, C. F. (2017). Meteorological conditions associated with the onset of flash drought in the Eastern United States. Agricultural and Forest Meteorology, 247, 414–423. https://doi.org/10.1016/J.AGRFORMET.2017.08.031Giglio et al., 2013

Hoell, A., Perlwitz, J., & Eischeid, J. (2019). The Causes, Predictability, and Historical Context of the 2017 U.S. Northern Great Plains Drought. https://www.drought.gov/drought/sites/drought.gov.drought/files/2017-NGP-drought-assessment.pdf

Keenan, T. F., Darby, B., Felts, E., Sonnentag, O., Friedl, M. A., Hufkens, K., O'Keefe, J., Klosterman, S., Munger, J. W., Toomey, M., & Richardson, A. D. (2014). Tracking forest phenology and seasonal physiology using digital repeat photography: A critical assessment. Ecological Applications, 24(6), 1478–1489. https://doi.org/10.1890/13-0652.1

Kolus, … Fisher, J.B. et al. Land carbon models underestimate the severity and duration of drought's impact on plant productivity. Sci Rep 9, 2758 (2019).

Li X and Xiao J (2019) A global, 0.05-degree product of solar-induced chlorophyll fluorescence derived from OCO-2, MODIS, and reanalysis data Remote Sens. 11

Osman, M., Zaitchik, B. F., Badr, H. S., Christian, J. I., Tadesse, T., Otkin, J. A., & Anderson, M. C. (2021). Flash drought onset over the contiguous United States: sensitivity of inventories and trends to quantitative definitions. Hydrology and Earth System Sciences, 25(2), 565–581. https://doi.org/10.5194/hess-25-565-2021

Osman, M., Zaitchik, B. F., Badr, H. S., Otkin, J., Zhong, Y., Lorenz, D., Anderson, M., Keenan, T. F., Miller, D. L., Hain, C., & Holmes, T. (2022). Diagnostic Classification of Flash Drought Events Reveals Distinct Classes of Forcings and Impacts. Journal of Hydrometeorology, 23(2), 275–289. https://doi.org/10.1175/JHM-D-21-0134.1

Otkin, J. A., M. C. Anderson, C. Hain, I. Mladenova, J. Basara, and M. Svoboda, 2013: Examining flash drought development using the thermal infrared based evaporative stress index. J. Hydrometeor., 14, 1057–1074

Otkin, J. A., Svoboda, M., Hunt, E. D., Ford, T. W., Anderson, M. C., Hain, C., & Basara, J. B. (2018). Flash droughts: A review and assessment of the challenges imposed by rapid-onset droughts in the United States. Bulletin of the American Meteorological Society, 99(5), 911-919.

Madani, N., Kimball, J. S., Parazoo, N. C., Ballantyne, A. P., Tagesson, T., Jones, L. A., Reichle, R. H., Palmer, P. I., Velicogna, I., Bloom, A. A., Saatchi, S., Liu, Z., & Geruo, A. (2020). Below-surface water mediates the response of African forests to reduced rainfall. *Environmental Research Letters*, *15*(3), 34063. https://doi.org/10.1088/1748-9326/ab724a

Madani, N., Parazoo, N. C., Kimball, J. S., Reichle, R. H., Chatterjee, A., Watts, J. D., Saatchi, S., Liu, Z., Endsley, A., Tagesson, T., Rogers, B. M., Xu, L., Wang, J. A., Magney, T., & Miller, C. E. (2021). The Impacts of Climate and Wildfire on Ecosystem Gross Primary Productivity in Alaska. *Journal of Geophysical Research: Biogeosciences*, *126*(6), e2020JG006078. https://doi.org/https://doi.org/10.1029/2020JG006078

McEvoy, D. J., Huntington, J. L., Hobbins, M. T., Wood, A., Morton, C., Anderson, M., & Hain, C. (2016). The evaporative demand drought index. Part II: CONUS-wide assessment against common drought indicators. Journal of Hydrometeorology, 17(6), 1763–1779. https://doi.org/10.1175/JHM-D-15-0122.1

Mo, K. C., & Lettenmaier, D. P. (2015). Heat wave flash droughts in decline. Geophysical Research Letters, 42(8), 2823–2829. https://doi.org/10.1002/2015gl064018

Mo, K. C., & Lettenmaier, D. P. (2016). Precipitation Deficit Flash Droughts over the United States. Journal of Hydrometeorology, 17(4), 1169–1184. https://doi.org/10.1175/jhm-d-15-0158.1

Mohammadi, K., Y. Jang, G. Wang (2022) Flash drought early warning based on the trajectory of solar-induced chlorophyll fluorescence, 119 (32) e2202767119. https://doi.org/10.1073/pnas.2202767119.

Parazoo, N. C., Bowman, K., Fisher, J. B., Frankenberg, C., Jones, D. B. A., Cescatti, A., Pérez-Priego, Ó., Wohlfahrt, G., & Montagnani, L. (2014). Terrestrial gross primary production inferred from satellite fluorescence and vegetation models. *Global Change Biology*, *20*(10), 3103–3121. https://doi.org/10.1111/gcb.12652

Parazoo, N. C., Barnes, E., Worden, J., Harper, A. B., Bowman, K. B., Frankenberg, C., Wolf, S., Litvak, M., & Keenan, T. F. (2015). Global Biogeochemical Cycles in the Texas-northern Mexico region. *Global Biogeochemical Cycles*, *29*, 1–19. https://doi.org/10.1002/2015GB005125.Received

Pascolini-Campbell, M., Fisher, J. B., & Reager, J. T. (2021). GRACE-FO and ECOSTRESS synergies constrain fine-scale impacts on the water balance. Geophysical Research Letters, 48(15), e2021GL093984.

Pendergrass, A. G., Meehl, G. A., Pulwarty, R., Hobbins, M., Hoell, A., AghaKouchak, A., Bonfils, C. J. W., Gallant, A. J. E., Hoerling, M., Hoffmann, D., Kaatz, L., Lehner, F., Llewellyn, D., Mote, P., Neale, R. B., Overpeck, J. T., Sheffield, A., Stahl, K., Svoboda, M., … Woodhouse, C. A. (2020). Flash droughts present a new challenge for subseasonal-to-seasonal prediction. *Nature Climate Change, 10*(3), 191–199. https://doi.org/10.1038/s41558-020-0709-0

Reichle, R. H., Liu, Q., Koster, R. D., Crow, W. T., De Lannoy, G. J. M., Kimball, J. S., Ardizzone, J. V., Bosch, D., Colliander, A., Cosh, M., Kolassa, J., Mahanama, S. P., Prueger, J., Starks, P., & Walker, J. P. (2019). Version 4 of the SMAP Level-4 Soil Moisture Algorithm and Data Product. Journal of Advances in Modeling Earth Systems, 11(10), 3106–3130. https://doi.org/10.1029/2019MS001729

Rodell, M., Houser, P. R., Jambor, U., Gottschalck, J., Mitchell, K., Meng, C. J., Arsenault, K., Cosgrove, B., Radakovich, J., Bosilovich, M., Entin, J. K., Walker, J. P., Lohmann, D., &

Toll, D. (2004). The Global Land Data Assimilation System. Bulletin of the American Meteorological Society, 85(3), 381–394. https://doi.org/10.1175/BAMS-85-3-381

Smith, W. K., Biederman, J. A., Scott, R. L., Moore, D. J. P., He, M., Kimball, J. S., Yan, D., Hudson, A., Barnes, M. L., MacBean, N., Fox, A. M., & Litvak, M. E. (2018). Chlorophyll Fluorescence Better Captures Seasonal and Interannual Gross Primary Productivity Dynamics Across Dryland Ecosystems of Southwestern North America. Geophysical Research Letters, 45(2), 748–757. https://doi.org/10.1002/2017GL075922

Van Der Werf, G. R., Randerson, J. T., Giglio, L., Van Leeuwen, T. T., Chen, Y., Rogers, B. M., Mu, M., Van Marle, M. J. E., Morton, D. C., Collatz, G. J., Yokelson, R. J., & Kasibhatla, P. S. (2017). Global fire emissions estimates during 1997-2016. *Earth System Science Data*, *9*(2), 697–720. https://doi.org/10.5194/essd-9-697-2017

Wolf, S., Eugster, W., Ammann, C., Häni, M., Zielis, S., Hiller, R., Stieger, J., Imer, D., Merbold, L., & Buchmann, N. (2013). Contrasting response of grassland versus forest carbon and water fluxes to spring drought in Switzerland. Environmental Research Letters, 8(3), 35007. https://doi.org/10.1088/1748-9326/8/3/035007

Wolf, S., Keenan, T. F., Fisher, J. B., Baldocchi, D. D., Desai, A. R., Richardson, A. D., ... & Van Der Laan-Luijkx, I. T. (2016). Warm spring reduced carbon cycle impact of the 2012 US summer drought. Proceedings of the National Academy of Sciences, 113(21), 5880-5885.

Yuan, X., Wang, Y., Ji, P., Wu, P., Sheffield, J., & Otkin, J. A. (2023). A global transition to flash droughts under climate change. Science, 380(6641), 187-191.

Zhang Y, Joiner J, Alemohammad S H, Zhou S and Gentine P (2018) A global spatially contiguous solar-induced fluorescence (CSIF) dataset using neural networks Biogeosciences 15 5779–800

Zhang, M. and Yuan, X.: (2020) Rapid reduction in ecosystem productivity caused by flash droughts based on decade-long FLUXNET observations, Hydrol. Earth Syst. Sci., 24, 5579–5593

Zhao, M., Liu, Y., & Konings, A. G. (2022). Evapotranspiration frequently increases during droughts. Nature Climate Change, 1-7.